

Structure of the nucleon from electromagnetic timelike form factors

F. Iachello and Q. Wan

Center for Theoretical Physics, Sloane Physics Laboratory, Yale University, New Haven, Connecticut 06520-8120, USA

(Received 15 December 2003; published 21 May 2004)

Recent experimental data on spacelike and timelike form factors of the nucleon are analyzed in terms of a model with an intrinsic structure and a meson cloud. The calculations are in perfect agreement with spacelike proton data, but deviate drastically from spacelike neutron data at $Q^2 > 1$ (GeV/c)². We suggest that timelike data be used to understand this discrepancy. Analysis of timelike data shows excellent agreement with both proton and neutron data in the entire range of measured $q^2 = -Q^2$, $3.52 \leq q^2 \leq 15$ (GeV/c)² values.

DOI: 10.1103/PhysRevC.69.055204

PACS number(s): 13.40.Gp, 14.20.Dh

Recently, Jones *et al.* [1] and Gayou *et al.* [2] have reported measurements of the ratio of the electric to magnetic form factor of the proton $\mu_p G_{E_p}(Q^2)/G_{M_p}(Q^2)$ using the recoil polarization technique. These results differ markedly from data obtained by Rosenbluth separation [3]. However, they agree perfectly with a calculation [4] performed within the framework of a two component model with an intrinsic part with form factor $g(Q^2)$ and a meson cloud parametrized in terms of vector mesons (ρ, ω, ϕ), Fig. 1. Very recently, Madey *et al.* [5] have reported measurements of the ratio of electric to magnetic form factors of the neutron $\mu_n G_{E_n}(Q^2)/G_{M_n}(Q^2)$, again using the the recoil polarization method, which agree with the calculation up to $Q^2 \sim 0.7$ (GeV/c)² but disagree from there on. Data for $G_{M_n}(Q^2)$ obtained with Rosenbluth separation also agree with the calculation up to 1 (GeV/c)² but disagree from there on, Fig. 2. As pointed out recently by Tomasi-Gustafsson and Rekalo [6], a comprehensive model of nucleon structure must simultaneously describe proton and neutron, and form factors both in the spacelike and timelike region. We therefore suggest that timelike form factors be used to test unified descriptions of nucleon structure. Timelike form factors can be obtained from the spacelike form factors theoretically by analytic continuation and experimentally from $e^+e^- \rightarrow p\bar{p}$, $e^+e^- \rightarrow n\bar{n}$, and $p\bar{p} \rightarrow e^+e^-$ reactions. In this paper, after a brief review of the situation for spacelike form factors, we calculate timelike form factors and compare with available data. The agreement between experiment and theory both for proton and neutron magnetic form factors is excellent. A test of our (and other) calculations that could be done in high luminosity e^+e^- colliders (Beijing, Frascati) provides an opportunity to unravel the structure of the nucleon, the fundamental building block of matter.

Two basic principles play a crucial role in the analysis of electromagnetic form factors of the nucleon. The first is relativistic invariance. This principle fixes the form of the nucleon current to be

$$J^\mu = F_1(Q^2)\gamma^\mu + \frac{\kappa}{2M_N}F_2(Q^2)i\sigma^{\mu\nu}q_\nu, \quad (1)$$

where $F_1(Q^2)$ and $F_2(Q^2)$ are the so-called Dirac and Pauli form factors and κ is the anomalous magnetic moment. This symmetry is expected to be exact. The second is isospin invariance. Although this symmetry is not exact, it is expected to be only slightly broken in a realistic theory of strong interaction. Isospin invariance leads to the introduction of isoscalar F_1^S and F_2^S and isovector F_1^V and F_2^V form factors and hence to relations among proton and neutron form factors. The observed Sachs form factors G_E and G_M can be obtained by the relations

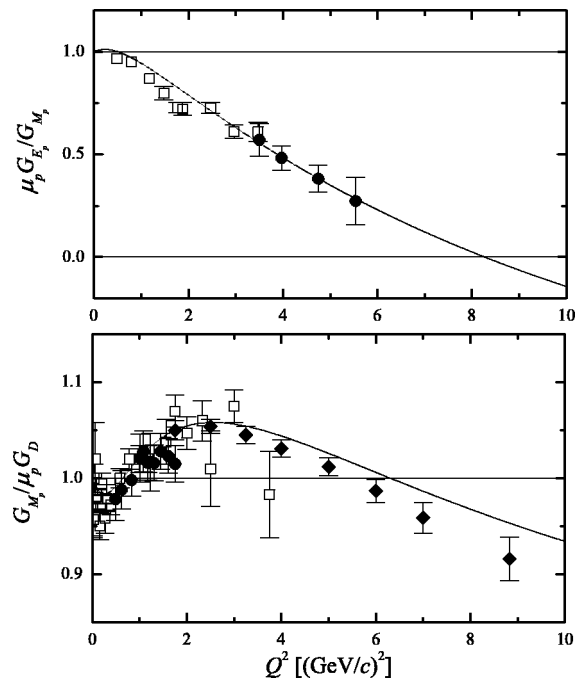


FIG. 1. Top panel: The measured ratio $\mu_p G_{E_p}/G_{M_p}$ compared with calculation. Reference [1]: open square, Ref. [2]: filled circle. Bottom panel: Experimental values $G_{M_p}/\mu_p G_D$ compared with calculation. Reference [9]: open square, Ref. [10]: filled circle, Ref. [3]: filled diamond.

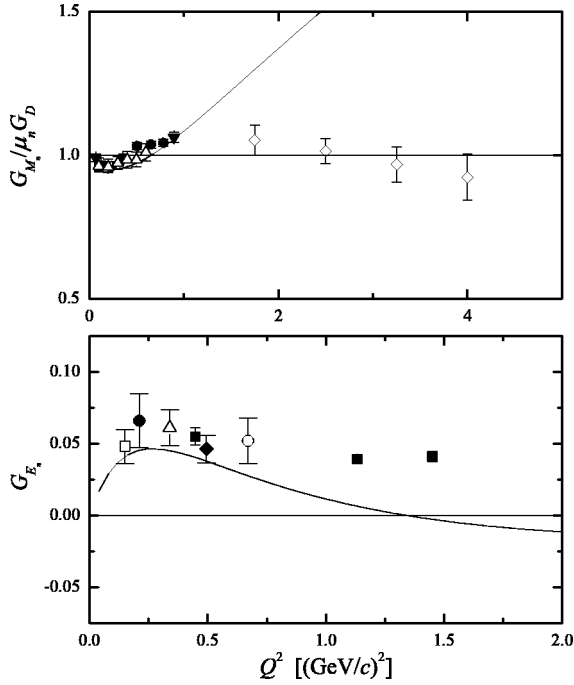


FIG. 2. Top panel: Selected experimental values for $G_{M_n}/\mu_n G_D$ compared with calculation. Reference [11]: open square, Refs. [12,13]: filled circle, Ref. [14]: filled down triangle, Refs. [15,16]: open up triangle, Ref. [17]: open diamond. Bottom panel: Selected experimental values for G_{E_n} compared with calculation. Reference [18]: open square, Ref. [19]: filled circle, Ref. [20]: filled diamond, Ref. [21]: open up triangle, Ref. [22]: open circle, Ref. [5]: filled square.

$$G_{M_p} = (F_1^S + F_1^V) + (F_2^S + F_2^V),$$

$$G_{E_p} = (F_1^S + F_1^V) - \tau(F_2^S + F_2^V),$$

$$G_{M_n} = (F_1^S - F_1^V) + (F_2^S - F_2^V),$$

$$G_{E_n} = (F_1^S - F_1^V) - \tau(F_2^S - F_2^V) \quad (2)$$

with $\tau = Q^2/4M_N^2$. Another important constraint is provided by perturbative QCD (PQCD) [7]. In leading order, in the limit $Q^2 \rightarrow \infty$, one expects $F_1 \propto 1/Q^4$ and $F_2 \propto 1/Q^6$.

Different models of the nucleon correspond to different assumptions for the Dirac and Pauli form factors. In 1973 a model of the nucleon in which the external photon couples to both an intrinsic structure, described by the form factor $g(Q^2)$ and a meson cloud, treated within the framework of vector meson dominance (ρ, ω, φ) was suggested [8]. In this model the Dirac and Pauli form factors are parametrized as

$$F_1^S(Q^2) = \frac{1}{2}g(Q^2) \left[(1 - \beta_\omega - \beta_\varphi) + \beta_\omega \frac{m_\omega^2}{m_\omega^2 + Q^2} + \beta_\varphi \frac{m_\varphi^2}{m_\varphi^2 + Q^2} \right],$$

$$F_1^V(Q^2) = \frac{1}{2}g(Q^2) \left[(1 - \beta_\rho) + \beta_\rho \frac{m_\rho^2}{m_\rho^2 + Q^2} \right],$$

$$F_2^S(Q^2) = \frac{1}{2}g(Q^2) \left[(-0.120 - \alpha_\varphi) \frac{m_\omega^2}{m_\omega^2 + Q^2} + \alpha_\varphi \frac{m_\varphi^2}{m_\varphi^2 + Q^2} \right],$$

$$F_2^V(Q^2) = \frac{1}{2}g(Q^2) \left[3.706 \frac{m_\rho^2}{m_\rho^2 + Q^2} \right]. \quad (3)$$

In Ref. [8] three forms of the intrinsic form factor $g(Q^2)$ were used. The best fit was obtained for $g(Q^2) = (1 + \gamma Q^2)^{-2}$. This form is consistent with PQCD and will be used in the remaining part of this article. Before comparing with the data, an additional modification is needed. In view of the fact that the ρ meson has a non-negligible width, one needs to replace [8]

$$\frac{m_\rho^2}{m_\rho^2 + Q^2} \rightarrow \frac{m_\rho^2 + 8\Gamma_\rho m_\pi/\pi}{m_\rho^2 + Q^2 + (4m_\pi^2 + Q^2)\Gamma_\rho \alpha(Q^2)/m_\pi}, \quad (4)$$

where

$$\alpha(Q^2) = \frac{2}{\pi} \left[\frac{4m_\pi^2 + Q^2}{Q^2} \right]^{1/2} \ln \left(\frac{\sqrt{4m_\pi^2 + Q^2} + \sqrt{Q^2}}{2m_\pi} \right). \quad (5)$$

This replacement is important for small Q^2 , although, because of the logarithm dependence of the $\pi\pi$ cut expressed by the function $\alpha(Q^2)$, its effect is felt even at moderate and large Q^2 .

By using the coupling constants given in Table I of Ref. [8] $\beta_\rho=0.672, \beta_\omega=1.102, \beta_\varphi=0.112, \alpha_\varphi=-0.052$, an intrinsic form factor with $\gamma=0.25 (\text{GeV}/c)^{-2}$, standard values of the masses ($m_\rho=0.765 \text{ GeV}, m_\omega=0.784 \text{ GeV}, m_\varphi=1.019 \text{ GeV}$) and a ρ width $\Gamma_\rho=0.112 \text{ GeV}$, one can calculate all form factors. The results are shown in Figs. 1 and 2. The calculation is in excellent agreement with the ratio $\mu_p G_{E_p}(Q^2)/G_{M_p}(Q^2)$, as measured recently by the recoil polarization method (Fig. 1, top panel). The calculation is also in excellent agreement with measurements of $G_{M_p}(Q^2)$ (Fig. 1, bottom panel) up to the largest measured value $Q^2 \approx 9 (\text{GeV}/c)^2$. For convenience of presentation the values of G_M have been normalized to the so-called dipole form factor $G_D = (1 + Q^2/0.71)^{-2}$. The situation for neutron form factors is different. In Fig. 2 top, the calculated values of $G_{M_n}(Q^2)/\mu_n G_D(Q^2)$ are compared with recent experiments up to $1 (\text{GeV}/c)^2$ and to older SLAC data for $Q^2 \geq 1 (\text{GeV}/c)^2$. As one can see, the calculation agrees perfectly with data below $1 (\text{GeV}/c)^2$ but it disagrees drastically with SLAC data at $Q^2 \geq 1 (\text{GeV}/c)^2$. While the calculation keeps increasing with increasing Q^2 the data decrease and drop below the dipole value. Preliminary (unpublished)

data from TJNAF also appear to indicate that G_{M_n}/G_D does not increase with Q^2 . In Fig. 2 bottom, recent experimental values for G_{E_n} are compared with the calculation. They agree with the calculation up to 0.7 GeV. However, TJNAF data on the ratio $\mu_n G_{E_n}(Q^2)/G_{M_n}(Q^2)$ just published [5], and shown as filled squares in Fig. 2 bottom, disagree with the calculation. While the calculation goes through zero at $Q^2 \approx 1.4$ (GeV/c)², the data remain positive and in fact increase with Q^2 .

Since our purpose here is to present results for timelike form factors, we do not elaborate further on spacelike data, but proceed to a calculation of timelike form factors. They can be obtained from the spacelike form factors by an appropriate analytic continuation. Within the framework of the model presented here, two ingredients are needed: (i) an analytic continuation of the intrinsic form factor $g(Q^2)$ and (ii) an analytic continuation of the vector meson form factors. For the intrinsic part, we do a simple analytic continuation that takes into account the complex nature of the $p\bar{p}$ interaction

$$g(q^2) = \frac{1}{(1 - \gamma e^{i\theta} q^2)^2}, \quad (6)$$

where $q^2 = -Q^2$. We take $\gamma = 0.25$ (GeV/c)⁻² as in the spacelike region, but we introduce, in the timelike region, a phase θ that takes into account annihilation channels. The calculation of θ from first principles (QCD) is a challenging problem that we do not address in the present article. As far as the meson component is concerned, the width of the ω and ϕ mesons is small and can be neglected. For the ρ meson, the replacement (4) becomes, in the timelike region $q^2 \geq 4m_\pi^2$ [23],

$$\frac{m_\rho^2}{m_\rho^2 - q^2} \rightarrow \frac{m_\rho^2 + 8\Gamma_\rho m_\pi / \pi}{m_\rho^2 - q^2 + (4m_\pi^2 - q^2)\Gamma_\rho \alpha(q^2)/m_\pi + i\Gamma_\rho 4m_\pi \beta(q^2)}, \quad (7)$$

where

$$\alpha(q^2) = \frac{2}{\pi} \left[\frac{q^2 - 4m_\pi^2}{q^2} \right]^{1/2} \ln \left(\frac{\sqrt{q^2 - 4m_\pi^2} + \sqrt{q^2}}{2m_\pi} \right),$$

$$\beta(q^2) = \sqrt{\frac{\left(\frac{q^2}{4m_\pi^2} - 1 \right)^3}{\frac{q^2}{4m_\pi^2}}}. \quad (8)$$

We note that the parametrization (2) satisfies the kinematical constraint $G_E(4M_N^2) = G_M(4M_N^2)$. Using the same parameters of the spacelike calculation and adjusting the angle θ , one obtains the proton magnetic form factor $|G_{M_p}(q^2)|$ shown in Fig. 3 top. The absolute value is used here since G_{M_p} is now complex. The calculation is compared with data. The angle θ obtained from a best fit is $\theta \approx 53^\circ$. The data from Fermilab Experiment E760 and E835 [29,30], extracted under the assumption $|G_{E_p}| = |G_{M_p}|$, have been corrected with our calculated $G_{E_p}(q^2)$ values. Data and calculation have

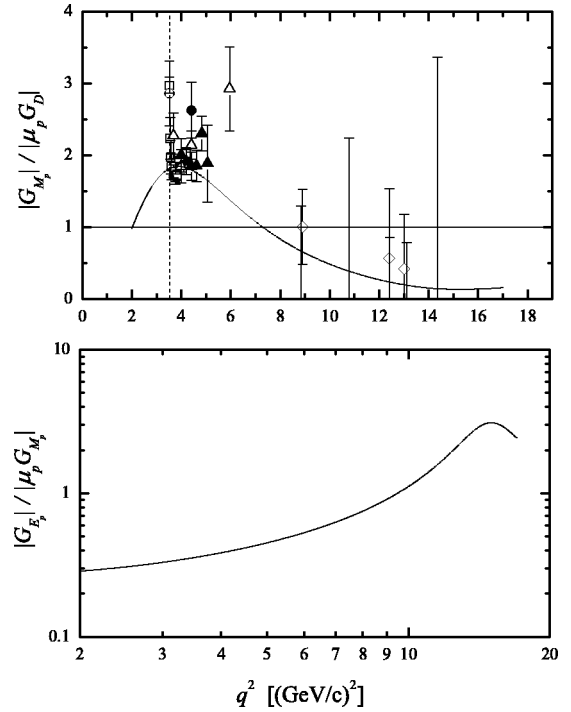


FIG. 3. Top panel: Experimental values for $|G_{M_p}|/|\mu_p G_D|$ compared with calculation. Reference [24]: filled circle, Ref. [25]: open circle, Ref. [26]: filled triangle, Ref. [27]: open square, Ref. [28]: open triangle, Ref. [29]: filled square, Ref. [30]: open diamond. Data from Fermilab Experiment E760 and E835 have been corrected with our calculated G_{E_p} values. Bottom panel: calculated ratio $|G_{E_p}|/|\mu_p G_{M_p}|$.

been normalized to the dipole form factor $G_D(q^2) = (1 - q^2/0.71)^{-2}$ for purposes of presentation. Apart from the threshold behavior, the agreement is good. Our predicted ratio $|G_{E_p}|/|\mu_p G_{M_p}|$ is shown in Fig. 3 bottom. As a consequence of the drop of G_{E_p} in the spacelike region, the ratio $|G_{E_p}|/|\mu_p G_{M_p}|$ increases with q^2 in the timelike region. No data exist on this ratio. It would be of the utmost importance to measure it. Without further parameters one can calculate the neutron magnetic form factor $G_{M_n}(q^2)$. A comparison with experiment [31], again normalized to the dipole, is shown in Fig. 4 top. The agreement is astonishing. In addition, we note that, as a consequence of the rise of G_{M_n} (Fig. 2, top) and the drop of G_{M_p} (Fig. 1, bottom) in the spacelike region, the ratio $|G_{M_n}|/|G_{M_p}|$ is calculated and observed to be ≈ 2 in the q^2 range 4–6 (GeV/c)². This is in marked disagreement with the $SU(6)$ value $|(-2/3)|$ but in agreement with PQCD that predicts $G_{M_p}/G_{M_n} \rightarrow 0^-$ as a power of $\ln(q^2/\Lambda^2)$ [32]. It would be of utmost importance to remeasure G_{M_n} to confirm this result. A similar conclusion was reached by Hammer, Meißner, and Drechsel [33] years ago, in a dispersion theoretical analysis [34] of spacelike and timelike. For future reference we also give in Fig. 4, bottom, our predicted ratio $|G_{E_n}|/|\mu_n G_{M_n}|$ needed for the extraction of G_{M_n} .

The comparison between data and calculation shows deviations in the threshold region $q^2 \geq 4M_N^2$. In order to understand these deviations, we have followed the suggestion of

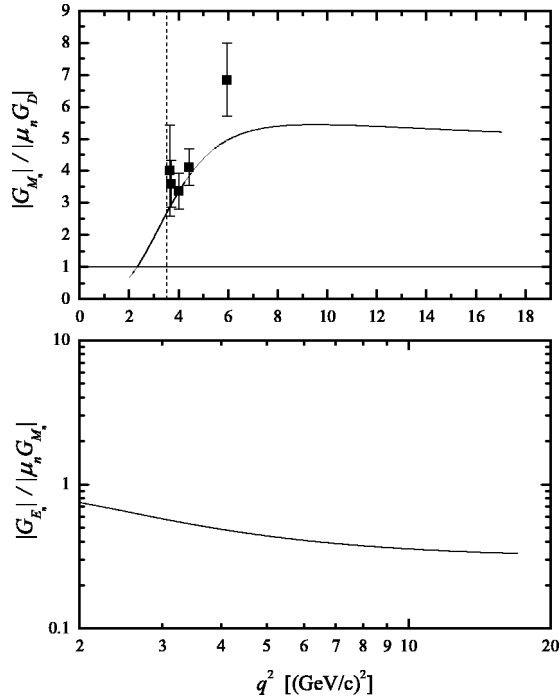


FIG. 4. Top panel: Experimental values for $|G_{M_n}|/|\mu_n G_D|$ compared with calculation. Reference [31]: filled square. Bottom panel: calculated ratio $|G_{E_1}|/|\mu_n G_{M_1}|$.

Ref. [31] and added to F_2 a subthreshold isoscalar resonance at $m_X=1.870$ (GeV/c^2) with negligible width $\Gamma_X=0$

$$F_2^S(q^2) = \frac{1}{2}g(q^2) \left[(-0.120 - \alpha_\varphi - \alpha_X) \frac{m_\omega^2}{m_\omega^2 - q^2} + \alpha_\varphi \frac{m_\varphi^2}{m_\varphi^2 - q^2} + \alpha_X \frac{m_X^2}{m_X^2 - q^2} \right]. \quad (9)$$

By using the coupling constant value $\alpha_X=0.001$ we obtain the results shown in Figs. 5 top and bottom. The addition of this very weakly coupled resonance has negligible effect on the spacelike form factor but a major effect on the timelike form factors near threshold. If the resonance is isovector and is added to F_2^V one obtains a similar result but with reversed behavior for neutron. We believe that these figures are strong evidence for the occurrence of a subthreshold resonance with $J^{PC}=1^{--}$ in $p\bar{p}$ and $n\bar{n}$.

In conclusion, we have performed an analysis of timelike form factors of the proton and neutron. Timelike data for both proton and neutron are in excellent agreement with a simple analytic continuation of the model of Ref. [8]. The combined spacelike and timelike calculations are in perfect agreement with all data except neutron spacelike data above $Q^2=1$ (GeV/c^2). These results suggest the following possible scenarios: (i) Additional contributions need to be added to the parametrization, (3). This has been investigated and its results will be present in a forthcoming publication [35]. (ii) The extraction of G_{M_n} from either of the two data sets, spacelike [17] and timelike [31], has problems. Spacelike and timelike form factors are related by analytic continuation.

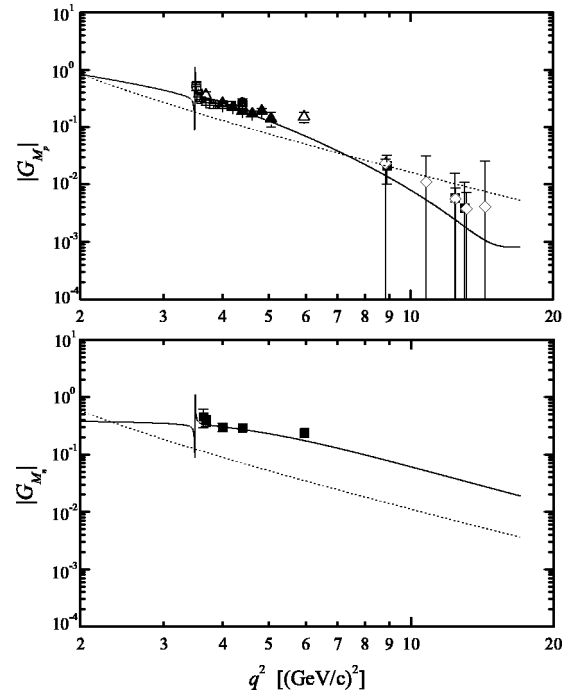


FIG. 5. Effect of an isoscalar subthreshold resonance on the form factors $|G_{M_p}|$ (top panel) and $|G_{M_n}|$ (bottom panel). The dotted line is the dipole form factor μG_D .

The experimental values of $|G_{M_n}|$ in the timelike region [at $q^2 \approx 4-5$ (GeV/c^2)] are a factor of 5–6 larger than G_{M_n} in the spacelike region [at $Q^2 = -q^2 \approx 4-5$ (GeV/c^2)]. A theorem on analytic functions [36] states that the asymptotic behavior of the form factors must be the same in the spacelike and timelike region. Although 4–5 (GeV/c^2) may not yet be in the asymptotic region, nonetheless the large discrepancy may indicate that one of the two sets of data suffers from major problems. It should be noted that a similar situation occurs from proton spacelike data, where the values of G_{E_p} extracted from Refs. [1,2], are different from those extracted from Ref. [3]. A considerable theoretical effort is presently devoted to understand this discrepancy, perhaps through two-photon contributions. To resolve the discrepancy between spacelike and timelike neutron form factors, the following proposals have been made: (a) Madey *et al.*, to extend neutron spacelike measurements to 4 (GeV/c^2) at JLab [37]; (b) Baldini *et al.* to upgrade DAΦNE at Frascati in order to measure G_{M_n} and G_{E_n} in the timelike region by $e^+e^- \rightarrow n\bar{n}$ [38].

This work was performed in part under DOE Grant No. DE-FG-02-91ER40608. After the completion of this work, we learned that a calculation of spin-polarization effects in the timelike region using the 1973 parametrization has been done by Brodsky, Carlson, Hiller, and Hwang [39]. We wish to thank Carl Carlson for discussions. We also wish to thank Rinaldo Baldini for bringing to our attention the neutron timelike data of Fig. 4 and for stimulating discussions, Egle Tomasi-Gustafsson for bringing to our attention [6], and Gianni Salme for bringing to our attention some of the data reported in Fig. 2.

- [1] M. K. Jones *et al.*, Phys. Rev. Lett. **84**, 1398 (2000).
- [2] O. Gayou *et al.*, Phys. Rev. Lett. **88**, 092301 (2002).
- [3] L. Andivahis *et al.*, Phys. Rev. D **50**, 5491 (1994).
- [4] F. Iachello, Eur. Phys. J. A **19**, 29 (2004).
- [5] R. Madey *et al.*, Phys. Rev. Lett. **91**, 122002 (2003).
- [6] E. Tomasi-Gustafsson and M. P. Rekalo, Phys. Lett. B **504**, 291 (2001).
- [7] G. P. Lepage and S. J. Brodsky, Phys. Rev. Lett. **43**, 545 (1979); Phys. Rev. D **22**, 2157 (1980).
- [8] F. Iachello, A. D. Jackson, and A. Lande, Phys. Lett. **43B**, 191 (1973).
- [9] W. Bartel *et al.*, Nucl. Phys. **B58**, 429 (1973).
- [10] P. E. Bosted *et al.*, Phys. Rev. C **42**, 38 (1990).
- [11] J. Golak *et al.*, Phys. Rev. C **63**, 034006 (2001).
- [12] H. Anklin *et al.*, Phys. Lett. B **336**, 313 (1994).
- [13] H. Anklin *et al.*, Phys. Lett. B **428**, 248 (1998).
- [14] G. Kubon *et al.*, Phys. Lett. B **524**, 26 (2002).
- [15] W. Xu *et al.*, Phys. Rev. Lett. **85**, 2900 (2000).
- [16] W. Xu *et al.*, Phys. Rev. C **67**, 012201(R) (2003).
- [17] A. Lung *et al.*, Phys. Rev. Lett. **70**, 718 (1993).
- [18] C. Herberg *et al.*, Eur. Phys. J. A **5**, 131 (1999).
- [19] I. Passchier *et al.*, Phys. Rev. Lett. **82**, 4988 (1999).
- [20] M. Ostrick *et al.*, Phys. Rev. Lett. **83**, 276 (1999).
- [21] D. Rohe *et al.*, Phys. Rev. Lett. **83**, 4257 (1999).
- [22] H. Zhu *et al.*, Phys. Rev. Lett. **87**, 081801 (2001).
- [23] W. R. Frazer and J. R. Fulco, Phys. Rev. **117**, 1609 (1960).
- [24] M. Castellano *et al.*, Nuovo Cimento **14**, 1 (1973).
- [25] G. Bassompierre *et al.*, Phys. Lett. **68B**, 477 (1977).
- [26] D. Bisello *et al.*, Nucl. Phys. **B224**, 379 (1983).
- [27] G. Bardin *et al.*, Nucl. Phys. **B411**, 3 (1994).
- [28] A. Antonelli *et al.*, Phys. Lett. B **334**, 431 (1994).
- [29] T. A. Armstrong *et al.*, Phys. Rev. Lett. **70**, 1212 (1993).
- [30] M. Ambrogiani *et al.*, Phys. Rev. D **60**, 032002 (1999).
- [31] A. Antonelli *et al.*, Nucl. Phys. **B517**, 3 (1998).
- [32] G. P. Lepage and S. J. Brodsky, Phys. Rev. Lett. **43**, 1625(E) (1979).
- [33] H.-W. Hammer, Ulf-G. Meißner, and D. Drechsel, Phys. Lett. B **385**, 343 (1996).
- [34] G. Höhler *et al.*, Nucl. Phys. **B114**, 505 (1976).
- [35] R. Bijker and F. Iachello (in preparation).
- [36] E. C. Titchmarsh, *Theory of Functions* (Oxford University Press, London, 1939), p. 179.
- [37] R. Madey *et al.*, JLab Proposal PR04-003.
- [38] R. Baldini *et al.* (private communication).
- [39] S. J. Brodsky, C. E. Carlson, J. R. Hiller, and D. S. Hwang, hep-ph/0310277.